



TEMPERATURE-DEPENDENT DEBONDING RESISTANCE OF 316 STAINLESS STEEL, INCONEL 625, AND TI-6AL-4V ALLOYS

Volkan ARIKAN^{1*}


¹Osmaniye Korkut Ata University, Faculty of Engineering, Department of Mechanical Engineering, 80000, Osmaniye, Türkiye

Abstract: This study investigates the temperature-dependent debonding properties of 316 Stainless Steel (SS), Inconel 625, and Ti-6Al-4V alloys in additive manufacturing using the finite element method. The analysis reveals notable relations between in mechanical properties and debonding resistance among these materials. Inconel 625 demonstrates superior performance at elevated temperatures, while SS and Ti-6Al-4V alloys show earlier degradation. Regarding debonding resistance, Inconel 625 performs comparably to SS and Ti-6Al-4V alloys, with Ti-6Al-4V exhibiting consistent resistance below 500 °C. SS, however, experiences a rapid loss of debonding resistance at lower temperatures. These findings provide valuable insights for material selection and design optimization in additive manufacturing. Further research can expand our understanding of these materials' behavior under different temperature regimes using the finite element method, enhancing their application potential.

Keywords: Debonding resistance, Finite element, Additive manufacturing

*Corresponding author: Osmaniye Korkut Ata University, Faculty of Engineering, Department of Mechanical Engineering, 80000, Osmaniye, Türkiye

E mail: volkanarikan@osmaniye.edu.tr (V. ARIKAN)

Volkan ARIKAN  <https://orcid.org/0000-0002-6102-6584>

Received: June 11, 2023

Accepted: July 01, 2023

Published: July 01, 2023

Cite as: Arıkan V. 2023. Temperature-dependent debonding resistance of 316 stainless steel, Inconel 625, and Ti-6Al-4V alloys. *BSJ Eng Sci*, 6(3): 287-294.

1. Introduction

Additive manufacturing is an innovative approach that holds a significant place in modern production processes. In this process, parts are built by layering materials on top of each other, enabling the creation of complex geometries and customized designs (Gu et al., 2021). The utilization of additive manufacturing spans across diverse industries such as automotive, aerospace, tooling, and manufacturing, among others. With the continuous advancement of this technology, it is expected that novel applications will arise in various industry sectors (Paul et al., 2020; Alzyod and Ficzer, 2021).

Additive manufacturing encompasses a wide range of metal materials, such as titanium alloys, nickel alloys, steel, and others (Niu et al., 2019; Abd-Elaziem et al., 2022). These metallic materials are extensively utilized in additive manufacturing technologies to produce functional parts of exceptional quality, with the materials available in powder, wire, or metal sheet forms. Specific examples of metal materials used in additive manufacturing processes include Ni-based alloys, Inconel 625, and Inconel 600 (Niu et al., 2019).

However, the mechanical properties of materials used in additive manufacturing can vary, especially with temperature changes. Within the Fused Filament Fabrication (FFF) additive manufacturing process, various building parameters, including nozzle temperature, print speed, and layer thickness, can exert an influence on not only the mechanical properties but also the surface wettability and morphology of the

fabricated object (Frascio et al., 2019). Furthermore, shape memory alloys (SMAs) and shape memory polymers (SMPs) exhibit distinct mechanical properties at different temperature ranges (Kitamura, 2021). It is also noteworthy that temperature fluctuations can impact the mechanical characteristics of piezocomposite materials employed in additive manufacturing (Omoni et al., 2021). Temperature is a critical factor in many industrial applications and affects the behavior of materials. This effect also influences the adhesive properties in the bonding region, resulting in different adhesive behaviors at different temperature ranges.

This necessitates a careful examination of the adhesive properties of materials used in additive manufacturing. Factors such as adhesive durability, bonding strength, and energy absorption can vary under different temperature conditions (Messmer et al., 2018; Yamazaki et al., 2020). Achieving reliable and robust adhesion is crucial for ensuring the structural integrity and performance of assembled components. Therefore, the selection, surface treatment (Zou et al., 2021) and application of adhesives should be guided by their ability to deliver optimal mechanical properties, durability, and long-term performance in varying operating conditions. This consideration plays a vital role in enhancing the overall safety, efficiency, and longevity of structures in these industries. Therefore, understanding and characterizing the temperature-dependent adhesive properties of materials is an essential step towards reliable and optimized additive manufacturing processes.



It is quite challenging to conduct experimental studies by combining all these factors. This difficulty has led to the widespread adoption of the finite element method in parametric studies. Finite element analysis (FEA) is a valuable tool for modeling and analyzing adhesive joints. ANSYS software is widely employed for FEA modeling of adhesive joints due to its extensive capabilities. FEA enables the examination of fracture behavior in adhesive joints and facilitates the modeling of cohesive zone behavior (Blackman et al., 2003). By utilizing FEA, engineers can gain insights into the structural integrity and performance of adhesive joints, helping to optimize their design and ensure reliable bonding in various applications.

In this article, we will investigate the temperature-dependent debonding properties of materials used in additive manufacturing numerically, exploring their significance and effects in more detail. We will also discuss the factors that influence the debonding performance of materials at different temperature ranges and how to manage these effects. This study aims to contribute to the enhancement of reliability and performance in additive manufacturing processes, providing valuable insights for practitioners in relevant industries.

2. Materials and Methods

In this study, the material selection process was conducted based on the specific requirements of the contact debonding analysis using the finite element method. Three distinct materials were carefully chosen to represent a range of commonly used alloys: 316 Stainless steel, Inconel 625, and Ti-6Al-4V. These materials were selected due to their widespread utilization in various industries, such as aerospace and automotive, where adhesive bonding is commonly employed. The mechanical properties of the selected materials are temperature-dependent. In order to understand the effects of changes in the mechanical properties of materials, it is assumed that the adhesive properties between the parts do not change with temperature. Table 1-3 summarizes the key mechanical properties, such as Young's modulus, Poisson's ratio at different temperature levels for each material (Alfano and Crisfield, 2001).

The finite element method (FEM) was employed as a powerful numerical tool to perform the contact debonding analysis. The ANSYS software package, renowned for its capabilities in structural analysis, was utilized for generating and solving the finite element models. The FEM analysis utilized a two-dimensional approach to capture the essential aspects of the contact debonding phenomenon accurately. The use of interface elements allows for the implementation of a bilinear cohesive zone model (CZM) in the analysis. In the case of Mode I loading dominance, the bilinear CZM model assumes that the separation of material interfaces is primarily influenced by the displacement jump

perpendicular to the interface. The relationship between the normal cohesive traction T_n and the normal displacement jump δ_n can be mathematically represented as follows (Alfano and Crisfield, 2001) (Equations 1 and 2);

Table 1. Temperature depended mechanical properties of 316 stainless steel

Temperature (°C)	Young's Modulus (MPa)	Poisson's Ratio
20	195000	0,25
100	191000	0,26
200	186000	0,275
300	180000	0,315
400	173000	0,33
500	164000	0,3
600	155000	0,32
700	144000	0,31
800	131000	0,24
900	117000	0,24
1000	100000	0,24

Table 2. Temperature depended mechanical properties of Inconel625

Temperature (°C)	Young's Modulus (MPa)	Poisson's Ratio
21	162000	0,278
537	124000	0,305
815	57000	0,33
982	38000	0,33
1093	21000	0,33

Table 3. Temperature depended mechanical properties of Ti-6Al-4V

Temperature (°C)	Young's Modulus (MPa)	Poisson's Ratio
20	107000	0,323
100	103400	0,328
200	99510	0,334
300	93710	0,339
400	85500	0,345
500	74710	0,351
600	61840	0,357
700	48160	0,363
800	35290	0,369
900	24500	0,374
1000	16290	0,38

$$T_n = K_n \delta_n (1 - D_n) \tag{1}$$

$$T_t = K_t \delta_t (1 - D_n) \tag{2}$$

where;

$K_{n,t}$ = normal and tangential cohesive stiffness
 $T_{n,t}$ = normal and tangential cohesive traction
 $\Delta_{n,t}$ = normal and tangential displacement jump
 D_n = Damage parameter

Finite element geometry prepared as 2D surface geometry and plane strain behavior selected. The prepared model consists of two plates with a length of 125 mm and a thickness of 2 mm, which are bonded to each other under the condition of bonded contact. In the analyses, the same materials have been used for both plates. The adhesion behavior between different materials could be a subject of a separate study. As an initial condition, two plates were bonded from neighbor edges, and one end edge was fixed with a fixed support while the lower and upper points of the other end edge were defined with a displacement of 10 mm. Schematic view of the model is given in Figure 1. The analysis setup encompassed a comprehensive consideration of various factors that can influence the contact debonding behavior. A minimum of 18 different temperature values were meticulously selected to investigate the effect of temperature on the contact debonding process. These

temperature values were chosen based on their relevance to the specific industrial applications targeted in this study.

An accurate mesh is of utmost importance for obtaining reliable and accurate results in finite element analysis. In this study, careful attention was given to the mesh generation process to ensure optimal representation of the geometry and contact interfaces. The mesh was refined strategically in regions of interest to capture the contact debonding phenomenon effectively. An 8-node quadratic (Quad8) Plane183 element was used as the element type in the model, resulting in a total of 2000 elements and 7018 nodes. The mesh element quality was achieved at a level of 100% for all elements (Figure 2).

After solving the finite element models, an extensive post-processing and result analysis were carried out to gain insights into the contact debonding behavior. The obtained results were thoroughly examined in terms of debonding patterns, stress distributions, peel stress, and other relevant parameters. Visualization tools and graphical representations were utilized to facilitate a comprehensive understanding of the analysis outcomes (Figure 3).

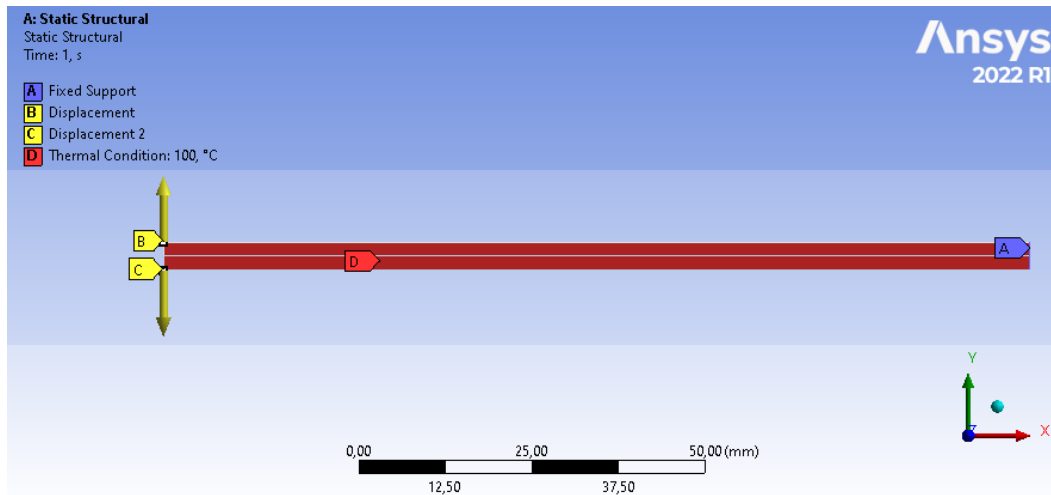


Figure 1. Initial and boundary conditions of the model.

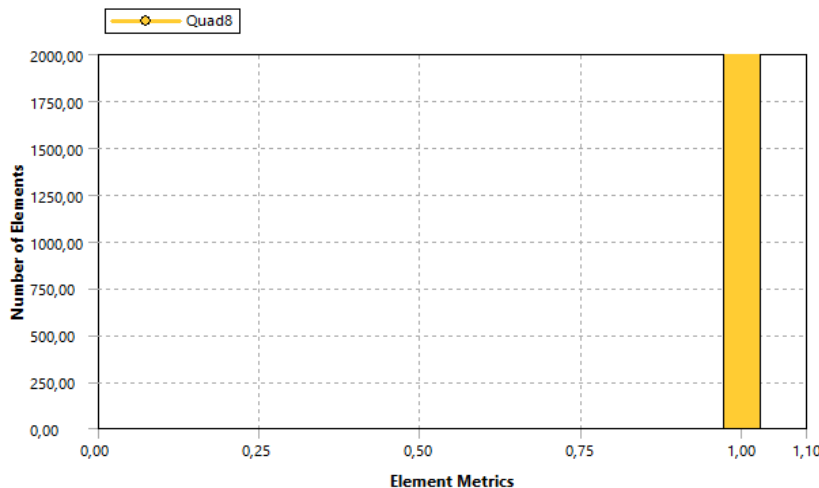


Figure 2. Element quality graph of mesh structure.

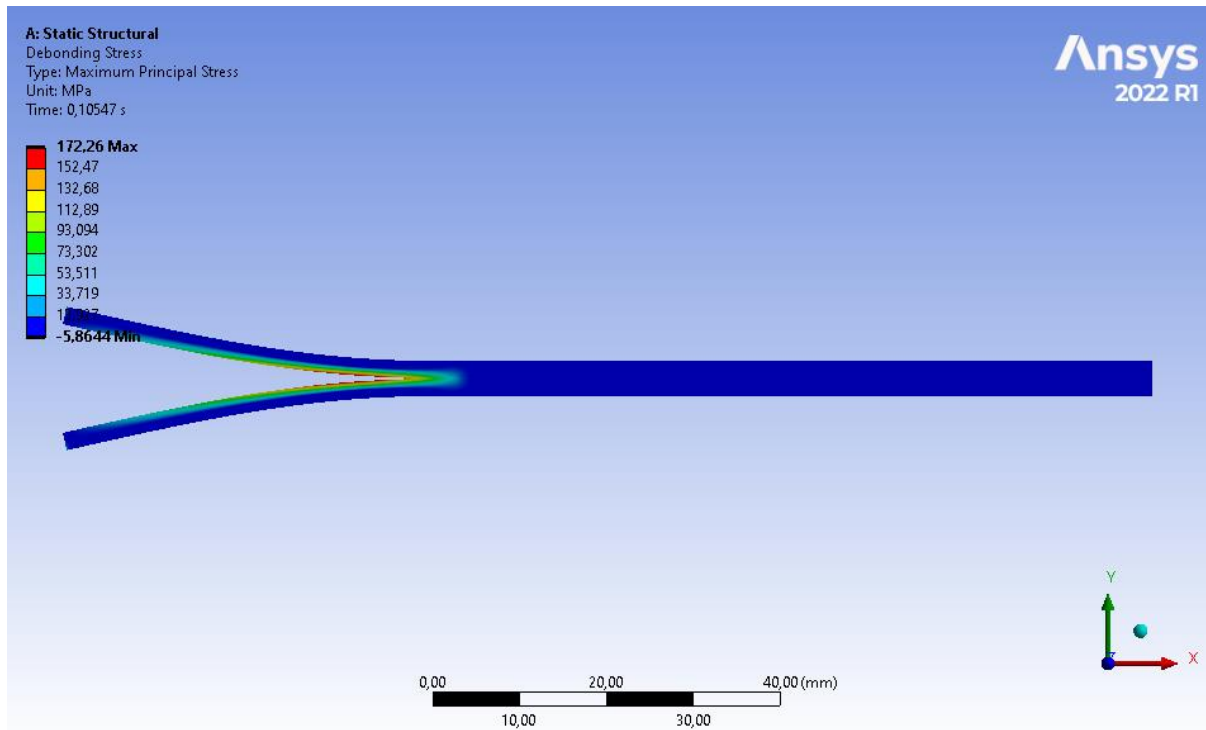


Figure 3. Stress distribution of sample debonding model at 0.1s.

3. Results and Discussion

In this section, the results of the contact debonding analysis and their implications will be discussed. The focus will be on the stress distribution during the separation of the bonded parts and the influence of temperature variations. Graphs and tables will be presented to illustrate these findings. Additionally, the results will be evaluated to provide insights into the debonding behavior.

316 Stainless Steel (SS), Inconel 625, and Ti-6Al-4V alloys were used in the study. When examined in terms of their mechanical properties, SS and Ti-6Al-4V materials exhibit a tendency of decreasing hardness and elastic modulus with increasing temperature, while Titanium shows a more stable fracture strength. Inconel 625 is a

nickel alloy commonly used at high temperatures, but its properties notably decrease, especially after 800 °C.

When evaluated in terms of thermal expansion coefficients, Inconel 625 stands out as the material with the highest coefficient, showcasing the best performance at high temperatures. The mechanical properties of SS and Ti-6Al-4V materials begin to weaken earlier with increasing temperature. Therefore, when examining the changes in debonding stress, the variations in material properties are also presented graphically.

Figures 4-6 present the temperature-dependent changes in Young's modulus, thermal expansion coefficient, and maximum stress observed at the adhesive interface during debonding for the SS material.

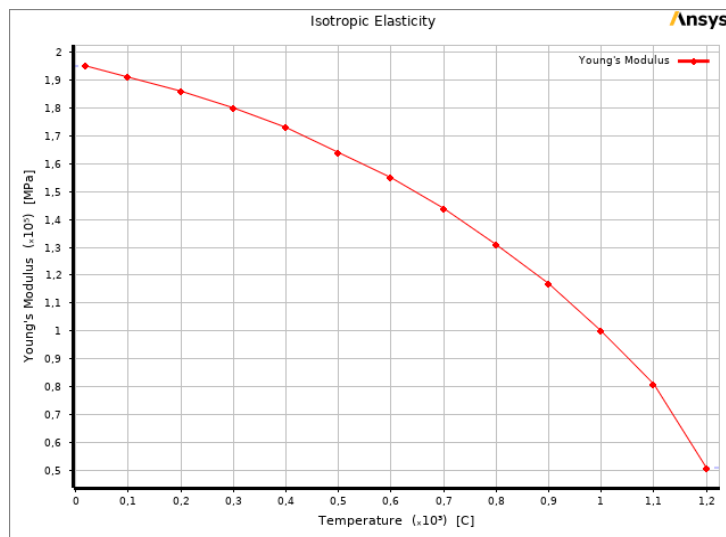


Figure 4. The temperature-dependent Young's modulus graph of 316 stainless steel.

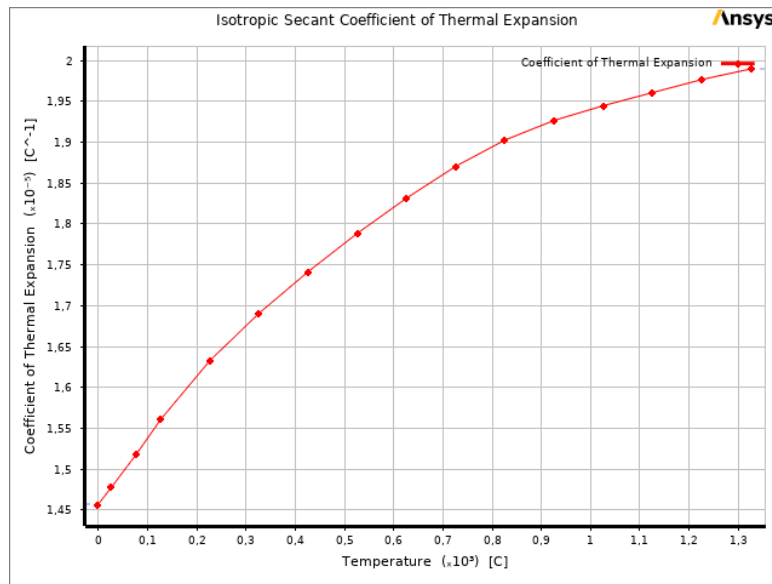


Figure 5. The temperature-dependent thermal expansion coefficient graph of 316 stainless steel.

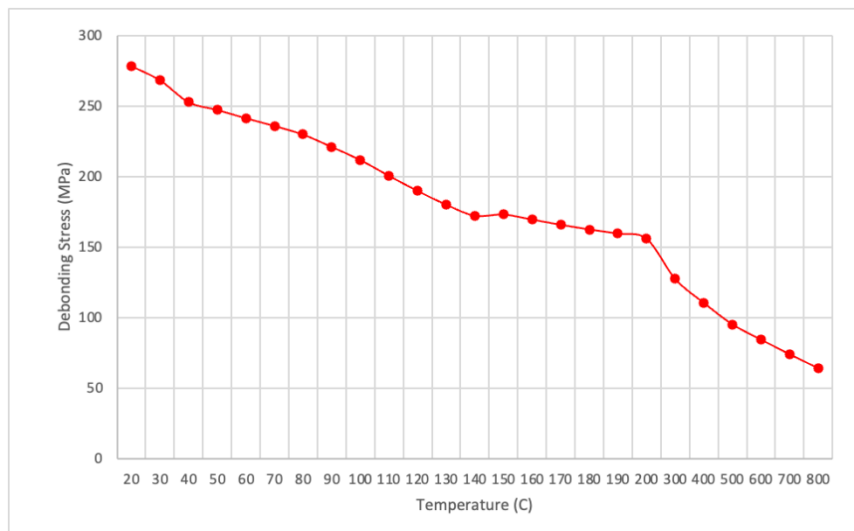


Figure 6. The temperature-dependent debonding stress graph of 316 stainless steel.

Upon analyzing the stress values, a dramatic decrease is observed between 100-300 °C, followed by a relatively stable trend. Hence, it can be stated that delamination becomes easier with increasing temperature. The changes in thermal expansion and Young's moduli, within the context of stress, indicate a sharp increase in the thermal expansion coefficient up to 300 °C, while Young's modulus decreases more rapidly starting from 500 °C. Figures 7-9 illustrate the temperature-dependent changes in Young's modulus, thermal expansion coefficient, and maximum stress observed at the adhesive interface during debonding for Inconel 625. Particularly, after 500 °C, both the thermal expansion coefficient and Young's modulus values exhibit a dramatic decrease. Inconel 625 experiences a significant reduction of debonding stress, approximately 62%, between 100-300 °C. However, beyond 500 °C, the debonding stress remains almost constant, ensuring the retention of peel strength.

For Ti-6Al-4V alloy, the corresponding graphs are presented in Figures 9-12. In contrast to SS and Inconel 625, the peel resistance of Ti-6Al-4V alloy shows a sharper decline after 500 °C. However, it exhibits a more stable peel resistance up to this temperature. When comparing these three materials, Inconel 625 demonstrates the best performance in terms of peel resistance. It maintains a peel resistance nearly equivalent to that of SS and Ti-6Al-4V alloys even at high temperatures. While Ti-6Al-4V alloy and SS perform similarly, the most notable difference between them is that Ti-6Al-4V alloy displays a balanced and resistant peel strength below 500 °C, whereas SS rapidly loses peel strength at lower temperatures. Thus, for working temperatures up to 500 °C, Ti-6Al-4V and Inconel 625 materials emerge as advantageous choices in terms of peel resistance.

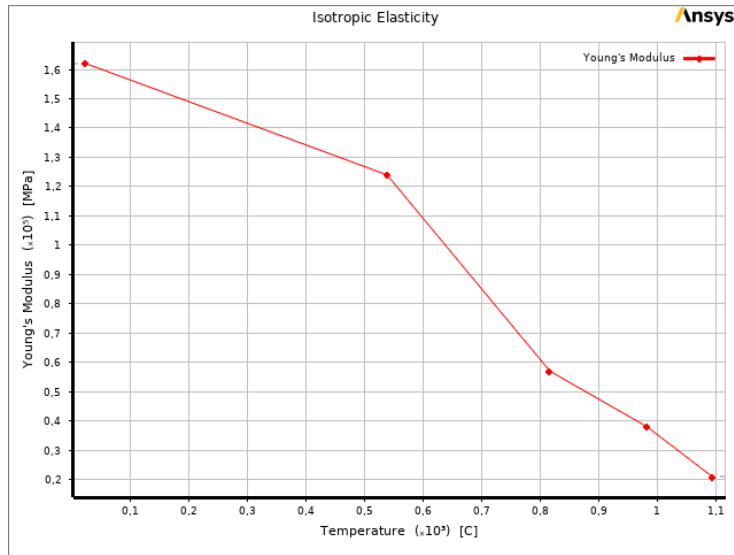


Figure 7. The temperature-dependent Young's modulus graph of Inconel 625.

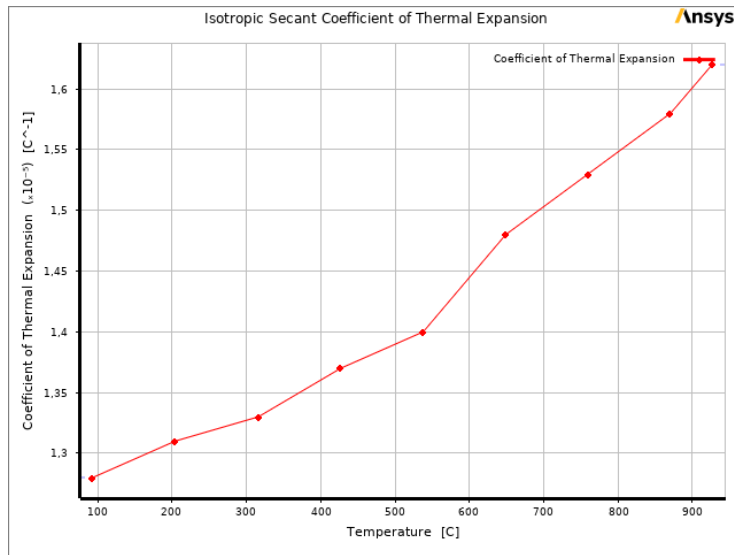


Figure 8. The temperature-dependent thermal expansion coefficient graph of Inconel 625.

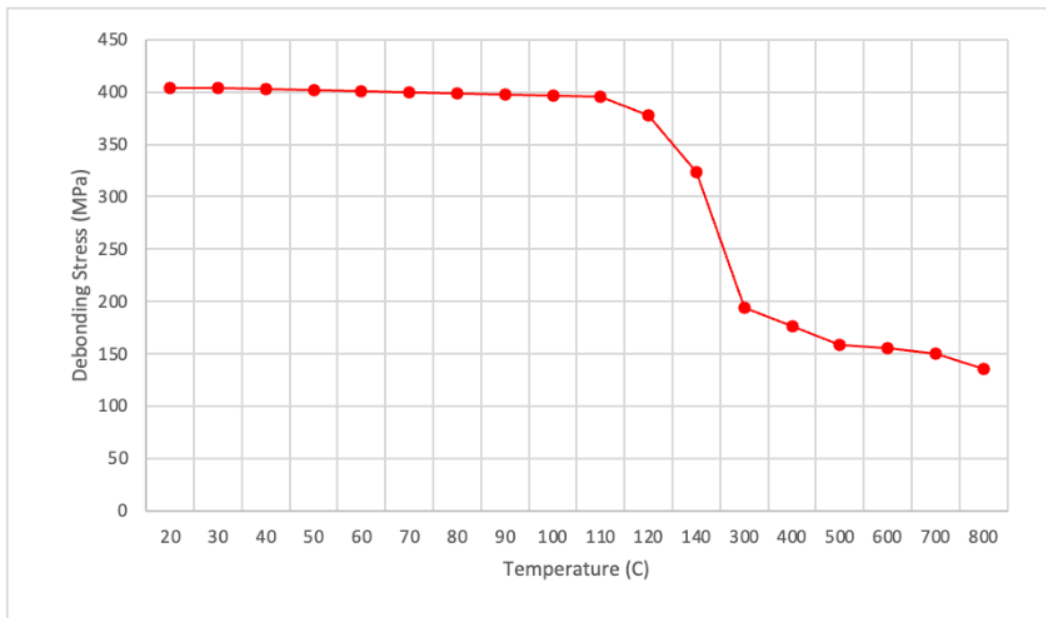


Figure 9. The temperature-dependent debonding stress graph of Inconel 625.

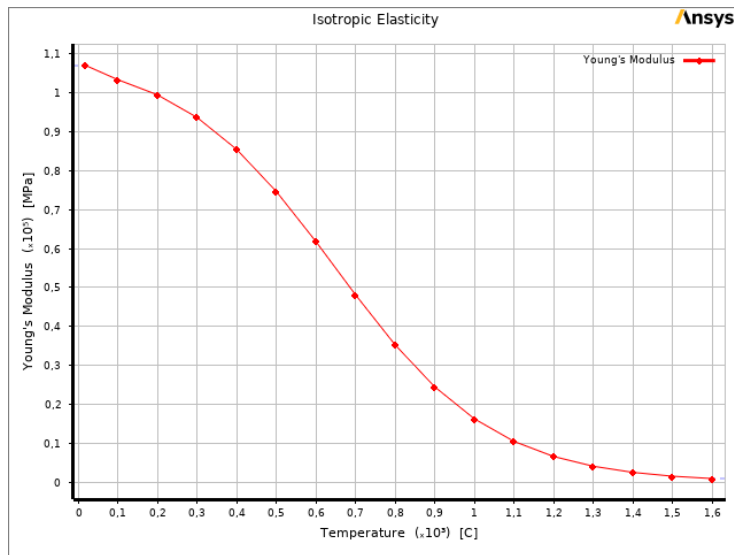


Figure 10. The temperature-dependent Young's modulus graph of Ti-6Al-4V alloy.

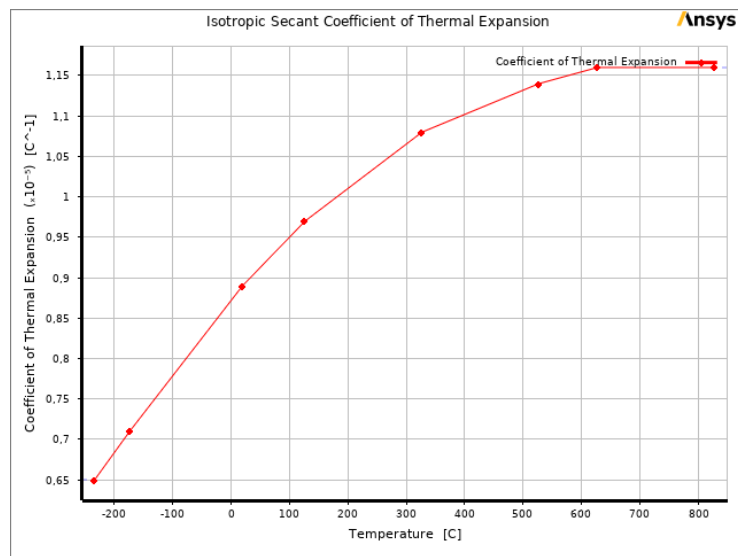


Figure 11. The temperature-dependent thermal expansion coefficient graph of Ti-6Al-4V alloy.

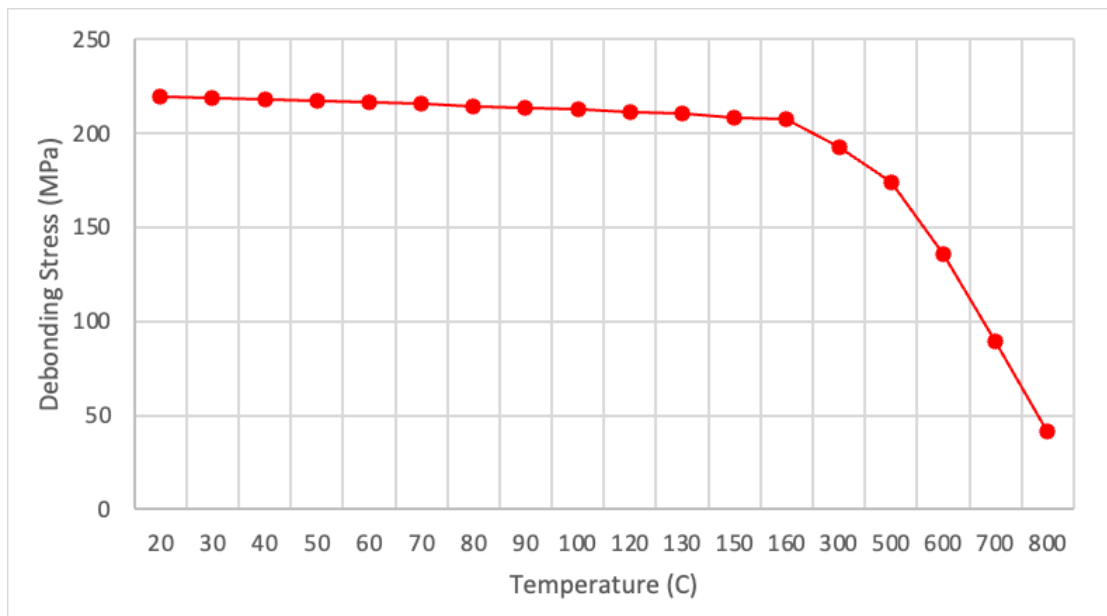


Figure 12. The temperature-dependent debonding stress graph of Ti-6Al-4V alloy.

4. Conclusion

The conducted study focused on analyzing the debonding stress of 316 Stainless Steel (SS), Inconel 625, and Ti-6Al-4V alloys in relation to temperature. The experimental findings revealed notable differences in the mechanical properties and peel resistance of these materials.

The evaluation of the coefficient of thermal expansion highlighted Inconel 625's superior performance at elevated temperatures, as it exhibited the highest value among the investigated materials. Conversely, SS and Ti-6Al-4V alloys demonstrated an earlier onset of mechanical property degradation with increasing temperature. Therefore, considering the variations in material properties is crucial when assessing debonding stress.

In terms of delamination resistance, Inconel 625 exhibited comparable performance to SS and Ti-6Al-4V alloys, even at high temperatures. While Ti-6Al-4V and SS showed similar behavior, Ti-6Al-4V displayed a more consistent and robust delamination resistance below 500 °C, while SS material rapidly lost its delamination resistance at lower temperatures. Consequently, Ti-6Al-4V and Inconel 625 materials emerge as advantageous choices for delamination resistance within the working temperature range of up to 500 °C.

In conclusion, this study provides valuable insights into the temperature-dependent mechanical properties and delamination resistance of 316 Stainless Steel, Inconel 625, and Ti-6Al-4V materials. The obtained results contribute to the understanding of material behavior in specific temperature ranges. Further research can be conducted to explore the mechanical properties of these materials under different temperature regimes, aiming to optimize their applications and enhance our knowledge in this field.

Author Contributions

The percentage of the author contributions is present below. The author reviewed and approved final version of the manuscript.

	V.A.
C	100
D	100
S	100
DCP	100
DAI	100
L	100
W	100
CR	100
SR	100
PM	100
FA	100

C=Concept, D= design, S= supervision, DCP= data collection and/or processing, DAI= data analysis and/or interpretation, L= literature search, W= writing, CR= critical review, SR= submission and revision, PM= project management, FA= funding acquisition.

Conflict of Interest

The author declared that there is no conflict of interest.

Ethical Consideration

Ethics committee approval was not required for this study because of there was no study on animals or humans.

References

Abd-Elaziem W, Elkatatny S, Abd-Elaziem AE, Khedr M, Abd El-baky MA, Hassan MA, Abu-Okail M, Mohammed M, Järvenpää A, Allam T, Hamada A. 2022. On the current research progress of metallic materials fabricated by laser powder bed fusion process: A review. *J Mater Res Tech*, 20: 681-707.

Alfano G, Crisfield MA. 2001. Finite element interface models for the delamination analysis of laminated composites: Mechanical and computational issues. *Int J Numer Methods Eng*, 50(7): 1701-1736.

Alzyod H, Ficzer P. 2021. Potential applications of additive manufacturing technologies in the vehicle industry. *Design Machin Struct*, 11(2): 5-13.

Blackman BRK, Hadavinia H, Kinloch AJ, Williams JG. 2003. The use of a cohesive zone model to study the fracture of fibre composites and adhesively-bonded joints. *Int J Fracture*, 119(1): 25-46.

Frascio M, Bergonzi L, Jilich M, Moroni F, Avalle M, Pirondi A, Monti M, Vettori M. 2019. Additive manufacturing process parameter influence on mechanical strength of adhesive joints, preliminary activities. *Acta Polytech CTU Proc*, 25: 41-47.

Gu D, Shi X, Poprawe R, Bourell DL, Setchi R, Zhu J. 2021. Material-structure-performance integrated laser-metal additive manufacturing. *Science*, 372(6545): eabg1487.

Kitamura K. 2021. Shape memory properties of Ti-Ni shape memory alloy / shape memory polymer composites using additive manufacturing. *Mater Sci Forum*, 1016: 697-701.

Messmer NR, Anjos EGR, Guerrini LM, Oliveira MP. 2018. Effect of geometry and hybrid adhesive on strength of finger joints of *Pinus elliottii* subject to humidity and temperature. *J Adhesion*, 94(8): 597-614.

Niu X, Singh S, Garg A, Singh H, Panda B, Peng X, Zhang Q. 2019. Review of materials used in laser-aided additive manufacturing processes to produce metallic products. *Front Mechanical Eng*, 14(3): 282-298.

Omoniyi OA, Mansour R, Cardona MJ, Briuglia ML, O'Leary RL, Windmill JFC. 2021. Fabrication and characterization of a novel photoactive-based (0–3) piezocomposite material with potential as a functional material for additive manufacturing of piezoelectric sensors. *J Mater Sci*, 32(9): 11883-11892.

Paul CP, Jinoop AN, Nayak SK, Paul AC. 2020. Laser additive manufacturing in industry 4.0: Overview, applications, and scenario in developing economies. *Add Manufac App Metals Composites*, 2020: 271-295. DOI: 10.4018/978-1-7998-4054-1.ch014.

Yamazaki D, Iwanami M, Isa M. 2020. Assessment of outdoor exposure effects on the long-term durability of epoxy resin adhesives used for steel-plate bonding. *J Adv Concrete Tech*, 18(8): 463-472.

Zou X, Huang L, Chen K, Jiang M, Zhang S, Wang M, Hua X, Shan A. 2021. Surface structuring via additive manufacturing to improve the performance of metal and polymer joints. *Metals*, 11(4): 567.